

# EXPERIMENTAL AND THEORETICAL INVESTIGATION OF PRESSURE TUBE CIRCUMFERENTIAL TEMPERATURE GRADIENTS DURING COOLANT BOIL-OFF \*

Q.M. Lei, D.B. Sanderson, M.L Swanson, G.A. Walters and H.E. Rosinger  
AECL Research - Whiteshell Laboratories  
Pinawa, Manitoba, Canada R0E 1L0

## ABSTRACT

A pressure-tube circumferential temperature distribution experiment under coolant boil-off conditions has been simulated using CATHENA (MOD-3.4a). The objectives of these simulations were to aid in the design of the experiment through pre-test simulations and to help in the analysis of the test results through post-test simulations.

The predicted results from the post-test simulations of the boil-off test generally agreed well with the experimental data. Predicted pressure-tube temperatures near the stagnant end of the test section compared well with the measured temperatures, typically being within 45°C or 6% of measured values prior to pressure-tube/calandria-tube ballooning contact. Measured and predicted pressure-tube temperatures at axial locations towards the steam exit end were good, however, not as good as near the stagnant end. This trend appeared to be related to the different local boil-off rates and the effect of the steam flowing towards the exit end. The general shape of the circumferential temperature distribution on the pressure tube during the boil-off transient, and the pressure-tube straining behaviour were well predicted. The predicted timing for the initial pressure-tube/calandria-tube contact was accurate to within 4 s near the stagnant end. The pressure tube was not predicted to fail in the post-test simulation, agreeing with experimental observations.

Comparative studies through numerical and experimental data plots are reported in this paper. This work was funded by the CANDU\*\* Owners Group (COG).

## 1. INTRODUCTION

Water in the horizontal fuel channels of a CANDU Pressurized Heavy-Water reactor may boil off slowly in some postulated loss-of-coolant accidents. This would expose the upper portion of the fuel bundle and pressure tube to superheated steam as the water level drops. The pressure tube would become hot at the top because of thermal radiation and steam convection while it remained near the saturation temperature below the liquid level. The resulting pressure-tube circumferential temperature gradient would induce localized thermal stresses and plastic deformation at the top of the pressure tube. Such

---

\* Presented at the 13th Annual Conference of Canadian Nuclear Society, Saint John, New Brunswick, June 7-10, 1992.

\*\* CANadian Deuterium Uranium, registered trademark of AECL.

conditions may cause nonuniform pressure-tube ballooning and the pressure tube could possibly rupture before coming into contact with the surrounding moderator-cooled calandria tube.

It is, therefore, necessary to study the circumferential temperature gradients and resultant deformation that can occur in a pressure tube subjected to stratified two-phase flow conditions. The data from such experimental studies are then used to validate fuel channel computer codes such as CATHENA [1] and SMARTT [2], which were designed to model the behaviour of a CANDU fuel channel under loss-of-coolant accidents (LOCAs). The experimental program was originally divided into four test series:

1. The Boil-Off Series (four tests) examined the temperature gradients and deformations that can develop on a pressure tube with stagnated coolant flow [3].
2. The Make-Up Water Series (five tests) examined the effects of constant water levels in the channel at differing conditions of power, liquid level, and pressure [4].
3. The Steam Cooling Series (three tests) examined the effects of steam flow on the thermal-mechanical behaviour of a fuel channel subjected to stratified two-phase flow.
4. The Variable Make-Up Water Series (three tests) examined the effects of controlled liquid levels more closely approximating postulated small LOCAs with impaired emergency core cooling.

In these tests, only one pressure-tube failure occurred as a result of circumferential temperature gradients that developed during the coolant boil-off. This occurred in the third test of the Boil-Off Series (S-1-3), which had a channel power of 36 kW/m and an internal pressure of 4 MPa. There were several other pressure-tube failures in this program. They were caused, however, by premature failures of the heater, i.e., the fuel element simulators (FESs). These failed fuel element simulators produced localized hot spots on the pressure tube that resulted in pressure-tube failures.

A supplementary test series using improved fuel element simulators was planned as a result of the above findings. The first test in this series (S-5-1) was a boil-off experiment at similar conditions as used in Test S-1-3 of the Boil-Off Series. The objectives of this paper are to outline the pre-test simulation results, and to document the CATHENA simulations that were performed as part of the post-test analysis of the experiment.

## 2. OVERVIEW OF THE CATHENA CODE

### 2.1 CATHENA

CATHENA [1] is a one-dimensional thermalhydraulics computer code developed at Whiteshell Laboratories primarily to analyse postulated loss-of-coolant accident scenarios for CANDU reactors. The code uses a nonequilibrium, two-fluid thermalhydraulic representation to describe two-phase fluid flow in piping networks. This results in a model where liquid and vapour phases may

have different pressures, velocities, and temperatures. Conservation equations for mass, momentum, and energy are solved for each phase (liquid and vapour). Interface mass, momentum and energy transfers are calculated using flow-regime-dependent constitutive relations obtained either from the literature or developed from separate-effects tests. The code uses a staggered-mesh, one-step, semi-implicit, finite-difference solution method which is not transit-time-limited. The heat-transfer package is general and allows the connection of multiple wall surfaces to a single thermalhydraulic node.

CATHENA has the ability to model a reactor channel in detail. The thermal responses of individual fuel pins within a bundle, the pressure tube and the calandria tube can be simulated in the axial, radial, and circumferential directions simultaneously. The effects of thermal radiation, zirconium-steam reaction, steam starvation, and the presence of noncondensables can all be included. As well, the ballooning and rupture of pressure tubes at high temperatures and the thermal effects of contacting metal surfaces, such as pressure-tube/calandria-tube contact, can be modelled.

The CATHENA code has been extensively validated against experimental results [1,5]. Quality assurance procedures for documentation, code modification, maintenance, and installation, as well as technical support for the use of the code, are exercised through the Thermalhydraulics Branch at Whiteshell Laboratories.

## 2.2 Modelling Assumptions

CATHENA was used to perform the pre- and post-test simulations for this experiment. The following assumptions were made for these simulations:

1. The test section was axially discretized into 12 equal-length segments. A 180-degree symmetry pin model was used to represent the fuel element simulator bundle, and each fuel element simulator was divided into four equal sectors. The half pressure and calandria tubes were each sectored into nine sectors (Figure 1).
2. Buoyancy-induced free convection in the steam within the pressure tube was approximated using a steam temperature distribution model.
3. Axial conduction and radiation were not modelled. Axial heat losses to the end fittings were neglected.
4. The emissivity of the fuel-element-simulator cladding was assumed to be constant at 0.6; the emissivities of the pre-oxidized pressure-tube inner and outer surfaces were assumed to be 0.8; and the emissivity of the calandria-tube inner surface was assumed to be 0.3.
5. The experimental spacers were not modelled in the simulations. Their effects on the prediction of local steam temperatures and channel flow resistances were assumed to be negligible.
6. The normalized power distributions were assumed to be 77.5, 89.4, and 111.1% for the inner, middle, and outer ring fuel element simulators, respectively.

Initial temperature conditions for the post-test simulations were taken from the experimental data. Electric power measured at the test section was used during the simulations.

### 2.3 Pressure-Tube Deformation Model Used in CATHENA

The CATHENA prediction of the pressure-tube deformation is implemented using the strain rate equations in the GRAD [6] program. At each time-step, CATHENA provides geometrical data as well as pressure and temperature information at each axial segment of the pressure tube. It then performs the strain calculation on each sector around the circumference of the pressure tube. The sector lengths, thicknesses, and pressure-tube diameter at that axial segment are then updated. There is at present no feedback to the thermalhydraulic and thermal radiation calculations as the flow area increases during ballooning.

This pressure-tube deformation model assumes that the pressure tube remains circular during ballooning. This results in pressure-tube/calandria-tube contact over the entire circumference when contact is predicted. Figure 2 depicts differences in the pressure-tube ballooning processes during a typical coolant boil-off experiment and the CATHENA idealization. The coolant boil-off causes the pressure tube to heat up nonuniformly and the pressure tube balloons in an egg-shaped pattern. The circular geometry assumption, however, may cause the predicted pressure-tube circumference to be larger than in the experiment prior to initial pressure-tube/calandria-tube contact. As a result, average transverse creep strains of the pressure tube could be overestimated during ballooning.

### 2.4 Pre-test Simulations

CATHENA (MOD-3.3h) was used to perform pre-test simulations for this experiment. Pre-test simulations were required to quantify the effect of the various changes made to the test section design (see Section 3.1) on the behaviour of the test section. Several pre-test simulations were performed using CATHENA, varying the test section power to match the pressure-tube heat-up rate of Test S-1-3 from the Boil-Off test series. The required bundle power was found to be 111 kW/m to achieve the desired heat-up rate of 5°C/s on the pressure tube. This bundle power was well in excess of the bundle power used in S-1-3 (36 kW/m) because of the increased mass of the new fuel element simulator bundle.

The pre-test simulations used an artificially large calandria tube to compensate for the nonconcentric deformation behaviour of the offset pressure tube. The intent of this numerical approximation was to force the top of the pressure tube to move 12.2 mm radially prior to contacting the calandria tube. This is roughly 3.6 mm more than it would have to move if the pressure tube was concentrically located in the calandria tube (Figure 1).

The use of a larger calandria-tube size, however, appeared too conservative for CATHENA simulations when the differences between pressure-tube deformations during an experiment and a simulation were examined.

Results from the final pre-test simulation for S-5-1 are summarized in Table 1. The code prediction used a bundle power of 200 kW (111 kW/m), which resulted in a peak pressure-tube heat-up rate of 5°C/s and a top-to-bottom temperature

gradient of 520°C around the pressure tube. The pressure tube was predicted to fail owing to excessive localized strain prior to calandria tube contact at a peak pressure-tube temperature of 773°C.

### 3. DESCRIPTION OF THE EXPERIMENT

#### 3.1 Experimental Apparatus

The 28-element test section consisted of three rings of fuel element simulators concentrically located inside an autoclaved Zr-2.5 Nb pressure tube (Figure 1). Each fuel element simulator consisted of Zircaloy-4 (Zr-4) cladding 15.2-mm OD and 14.4-mm ID, within which annular alumina pellets (14.3-mm OD, 6.1-mm ID, and 16 mm in length) electrically insulated the cladding from a graphite rod heater. The 6-mm-diameter graphite rod heaters were coated with tungsten carbide to minimize the reaction between the alumina and graphite at high temperatures. The length of the graphite rod heaters was 1800 mm.

The fuel element simulator design for this test was significantly different from previous fuel element simulator designs used in this series [3,4]. A comparison of test section differences required to accommodate these improved fuel element simulators is given in Table 2.

Five spacer plates, machined out of 0.90-mm-thick Zr-4, were symmetrically placed in the heated zone of the test section (Figure 1a). Their purpose was to simulate the effects of CANDU bundle end plates and to help minimize sag of the fuel element simulator bundle at high temperatures.

The fuel element simulator bundle used in S-5-1 was surrounded by a 2105-mm-long section of autoclaved Zr-2.5 Nb pressure tube mounted inside a 1780-mm-long Zr-2 calandria tube. The pressure tube was offset 3.6 mm in the calandria tube to represent a sagged pressure tube. The sagged pressure tube would result in a maximum deformation before it contacts the surrounding calandria tube. The test-section annulus (gap between the pressure and calandria tubes) contained an Inconel X-750 garter spring located at the test section centreline. This annulus was purged with CO<sub>2</sub> prior to the start of the experiment and a slow continuous purge of CO<sub>2</sub> was maintained throughout the experiment. The calandria tube was surrounded by heated, nonflowing water in an open tank. The top surface of the calandria tube was covered by at least 150 mm of water throughout the experiment.

One end of the pressure tube was closed to simulate flow stagnation. The other end of the pressure tube was opened to a vertical pipe (Figure 1a). This pipe was connected to a condenser and a surge tank that controlled the test section pressure.

#### 3.2 Instrumentation

The fuel element simulators were connected in parallel to a DC power supply. The power to the test section was determined using measured voltage drops across the test section and measured currents through the fuel element simulators. Power distribution throughout the fuel element simulator bundle was designed to be similar to that found in a Pickering-type fuel bundle.

Design targets for the normalized pin powers were 1.111, 0.894, and 0.775 for the outer, middle, and inner rings, respectively.

The heated length of the test section was instrumented at five distinct axial locations (Rings 1 to 5 in Figure 1a). Thermocouples were used to monitor temperatures of the fuel element simulator cladding, pressure and calandria tubes, exit steam, and moderator water. The thermocouples on the fuel element simulators and the pressure tube were 0.5-mm outer diameter Inconel-clad, K-type (chromel-alumel) with magnesium oxide insulation. The thermocouples on the calandria-tube surface were fiberglass insulated K-type with wire diameters of 0.13 mm. The thermocouples were installed by separating and spot-welding the sensing wires directly onto the appropriate surfaces.

Relative displacement of the pressure tube with respect to the calandria tube was monitored by top and bottom Linear Variable Differential Transformers (LVDTs) located near Ring 2, 455 mm from the closed end. A second LVDT was located on the top, near Ring 4, which was 1130 mm from the closed end.

### 3.3 Experimental Procedures

The water surrounding the calandria tube was heated to 75°C at the beginning of the test and the pressure tube was filled with water and pressurized to 4 MPa. The temperature of this pressurized water was gradually raised to the saturation temperature using 5 kW of electric power.

The test was started by opening the steam outlet valve and increasing the test section power to 200 kW (value based on pre-test simulations). The test was terminated when the pressure tube had fully ballooned into contact with the calandria tube.

### 3.4 Summary of the Experimental Results

The pressure-tube temperatures around the complete circumference at Ring 1 (225 mm from the closed end) were near the saturation temperature at the start of the full-power period (Figure 3). When the full power (about 200 kW) was applied, the water started to boil off and the temperatures at the top of the pressure tube increased once uncovered while the bottom of the pressure tube remained near the saturation temperature. A significant circumferential temperature gradient developed around the pressure tube as the water in the channel boiled off. No pressure-tube rupture or fuel element simulator failure occurred during this test. Some key results from Test S-5-1 are summarized in Table 1.

The average recorded pressure-tube heat-up rate at Ring 1 was 4°C/s. The temperatures of the pressure tube increased to a maximum of 760°C, just prior to ballooning into contact with the calandria tube at time = 714 s (Figure 3a). The pressure-tube to calandria-tube contact shorted out the thermocouples on the pressure tube, invalidating their results after ballooning contact. Temperature histories at other axial locations were similar to those at Ring 1, except that heat-up rates were slightly lower as one approached the steam exit end.

There existed a maximum axial pressure-tube temperature gradient of 50°C between Rings 1 and 4 (Figure 4), with temperatures at Ring 5 being slightly

higher than Ring 4. These axial temperature profiles reflect the effects of the local boil-off rates and the resultant steam flow produced. The steam cooling effect was minimal at Ring 1 since the steam velocities near the closed end were lower than the velocities at other locations.

Top-to-bottom circumferential temperature profiles that developed on the pressure tube at Rings 1 and 5 are shown in Figure 5. The maximum top-to-bottom temperature gradients on the pressure tube at Rings 1 and 5 were 475 and 420°C, respectively, just prior to initial ballooning contact.

Fuel element simulator cladding temperature histories at Ring 3 (675 mm from the closed end) are shown in Figure 6. The temperature increases on the cladding indicated the times when the fuel element simulator became dry. The corresponding thermocouple positions were then used to infer water levels in the pressure tube during the experiment. Peak cladding temperatures were not determined owing to premature failure of fuel-element-simulator thermocouples at around 1200°C.

Deformation of the pressure tube at Ring 2 (450 mm from the closed end) was monitored during the experiment by two LVDTs. The LVDT traces indicated a slight upward bowing of the pressure tube prior to ballooning (Figure 7). This early movement was caused by thermally induced bowing of the pressure tube as the top half of the pressure tube was considerably hotter than the bottom half. The pressure tube started to balloon when pressure-tube temperatures reached 650°C at time = 690 s, and made initial contact with the calandria tube at 714 s at Ring 1 and 719 s at Ring 2. The tube strained into full calandria-tube contact from the closed end to the steam-exit end over the following 10 s. The maximum pressure-tube temperature recorded prior to contact was 770°C (Table 1), occurring on the top at Ring 5. There was no pressure-tube failure in this experiment.

Post-test pressure-tube wall thicknesses at two axial locations are shown in Figure 8. These post-test wall thicknesses show a nonsymmetric deformation pattern with most of the straining occurring in the top half of the pressure tube. This pattern mirrors the top-to-bottom circumferential temperature gradients that were present on the pressure tube during ballooning.

#### 4. POST-TEST SIMULATIONS

##### 4.1 Overview

A simulation was performed as part of the post-test analysis of S-5-1 using CATHENA (MOD-3.4a). This simulation used actual calandria tube dimensions instead of the artificially large calandria tube used in the pre-test simulation, since the use of the larger calandria tube was found to be too conservative of an approximation of the offset pressure tube. The results of this post-test simulation are summarized in Table 1 and detailed comparisons with experimental results are presented in the following sections.

#### 4.2 Pressure-Tube Temperatures

Predicted and measured pressure-tube temperatures at three axial locations are discussed. Selected plots from two axial locations are shown in Figures 9 and 10.

Excellent agreement between measured and predicted results was found at Ring 1, 225 mm from the closed end of the pressure tube (Figure 9). Both measured and predicted temperatures increased as the water in the channel boiled off, exposing the pressure tube to radiation from the fuel element simulators. The measured pressure-tube temperatures on the top increased at an average rate of 4.0°C/s after 640 s, comparing favourably with the predicted heating rate of 4.5°C/s. Pressure-tube to calandria-tube contact was predicted to occur at Ring 1 at 710 s with a peak pressure-tube temperature of 765°C. This was in excellent agreement with the measured contact time of 714 s and contact temperature of 760°C.

The agreement between measured and predicted pressure-tube temperatures at axial locations further away from the sealed end of the pressure tube was good, however not as good as at Ring 1. Agreement between measured and predicted pressure-tube temperatures was good at Ring 3, 675 mm from the closed end. All temperatures around the pressure tube were predicted within 45°C (6%) prior to contact. Measured and predicted pressure-tube temperatures at Ring 5, 1425 mm from the closed end, agreed reasonably well (Figure 10). The temperature of the upper portion of the pressure tube was overestimated, especially in the early heat-up stage (near 600 s), by 60°C. This indicated the boil-off rate predicted at this location was slower than during the experiment. The discrepancy was probably due to not modelling the spacers used in the experiment, and the effects of steam flow to the exit end and axial heat losses to the end fittings.

Comparison between measured and predicted temperature distributions around the pressure tube at Rings 1 and 5 at four different times are shown in Figure 5. The successful prediction of these gradients is critical for the accurate prediction of local pressure-tube straining and the potential for pressure-tube rupture. Excellent agreement was achieved at Ring 1 and reasonably good agreement was found at Ring 5. A straight line was drawn between the measured temperature at the circumferential angle of 120 deg away from the top and the measured value at the bottom (180 deg) because there was no thermocouple between the two locations. Predicted temperatures, however, were fairly constant and close to the saturation temperature for the circumferential angles from 150 to 180 deg.

#### 4.3 Calandria-Tube, Steam and Cladding Temperatures

Comparison between measured and predicted calandria-tube temperatures at Ring 1 is shown in Figure 11a. Agreement between the two was reasonably good. CATHENA overestimated the peak calandria-tube temperature by 14°C as the pressure tube contacted the calandria tube. The overestimation may be due to the use of a high pressure-tube to calandria-tube contact conductance (8 kW/m<sup>2</sup>K) after ballooning contact.

The predicted steam exit temperatures (Figure 11b) compared favourably with measured data until the pressure tube started to balloon at 690 s. After that,

the measured and predicted values departed significantly. One reason for the discrepancy could be caused by the small amount of steam flowing through the exit pipe after 690 s. Most steam energy thereafter dissipated into the end fitting and the exit pipe during the experiment, resulting in cooler measured steam-exit temperatures. CATHENA assumed no thermal energy losses and thus continued to predict higher steam-exit temperatures even though small steam flow rates after 690 s were correctly predicted. Another possible cause is the effect of the increasing flow area resulting from ballooning of the pressure tube. This increased flow area would allow some of the steam to bypass the fuel element simulator bundle, resulting in significantly cooler steam exit temperatures. This flow bypass was not taken into account in the simulation.

Fuel-element-simulator cladding temperatures at Ring 3 (675 mm from the closed end) were well predicted (Figure 6). This indicated the fuel-element-simulator model and emissivity values used in this CATHENA simulation were proper.

#### 4.4 Pressure-Tube Ballooning

A comparison between measured and predicted pressure-tube ballooning at Ring 2 is given in Figure 7. CATHENA predicted the pressure tube to start ballooning at 690 s and contact the calandria tube 25 s later at 715 s. These compared well with the measured times of 690 and 719 s for the start of ballooning and initial calandria-tube contact.

The top of the pressure tube first contacted its calandria tube at 714 s along a narrow strip at Ring 1 during the experiment. Contact then spread axially and circumferentially over the next 10 s until the pressure tube had fully ballooned into calandria-tube contact. This nonuniform circumferential ballooning is not modelled in CATHENA as the code assumed the pressure tube remained circular during ballooning. This assumption resulted in simultaneous circumferential pressure-tube/calandria-tube contact at an axial location. In spite of this approximation, CATHENA adequately predicted variations in post-test wall thicknesses around the pressure tube (Figure 8a).

The corresponding true strains ( $\ln(w_0/w)$ , where  $w_0$  is the initial nominal wall thickness, 4.30 mm, and  $w$  is the current local wall thickness) are shown in Figure 8b. Agreement between measured and predicted values was reasonably good. A maximum strain of 59% on the top of the pressure tube was predicted, slightly higher than the measured value (51%) near the top.

## 5. DISCUSSION

CATHENA was used to perform pre- and post-test simulations of a Pressure-Tube Circumferential Temperature Distribution Experiment (S-5-1). The pre-test simulation results were used to plan the experiment as several design changes to the apparatus made it considerably different from the previous 15 tests in this program. The post-test simulations were performed as part of the post-test analysis of this experiment.

The pressure tube was predicted to fail prior to calandria-tube contact in the pre-test simulations. This simulation used an artificially large calandria tube in an attempt to compensate for the offset pressure tube used in the experiment. Closer analysis of this approximation, however, proved it to be

too conservative and, as a result, the assumption was not used for the post-test simulation.

The predicted pressure-tube temperatures near the stagnant end of the channel (Ring 1) compared well with measured temperatures. Predicted temperatures typically were within 45°C or 6% of measured values prior to ballooning contact. Measured and predicted pressure-tube temperatures at axial locations further away from the stagnant end were good, however, not as good as near the stagnant end. This trend appears to be related to the different local boil-off rates and the steam flow towards the exit end. At present, CATHENA does not adequately model this phenomena.

The circumferential temperature gradients on the pressure tube during coolant boil-off were reasonably well predicted. These top-to-bottom temperature gradients resulted in nonuniform deformation of the pressure tube. The pressure tube first contacted the calandria tube at the top and then the contact spread circumferentially until the entire pressure tube had contacted the calandria tube.

This nonuniform deformation behaviour was approximated in CATHENA. The code performs strain calculations on individual sectors around the pressure-tube circumference. The sector lengths, thicknesses, and resultant pressure-tube diameter are then updated. This deformation model can therefore calculate localized pressure-tube strain, but assumes the pressure tube remains circular. This results in pressure-tube/calandria-tube contact over the entire circumference when contact is predicted.

Despite this limitation, CATHENA accurately predicted pressure-tube ballooning and post-test pressure-tube wall thicknesses and resultant strains. The timing for the predicted pressure-tube/calandria-tube contact was between 4 to 14 s of the actual initial contact along different axial locations. The pressure tube was not predicted to fail in the post-test simulation, thus agreeing with experimental observations.

In general, good overall agreement between measurements and CATHENA predictions was found in this study. An in-depth comparison was made for pressure-tube and cladding temperatures, void fractions, steam temperatures, and pressure-tube deformation. All these comparisons showed that the assumptions made during this post-test simulation were appropriate.

A number of weaknesses in the CATHENA predictions were identified throughout this study. They are the circular geometry assumption made in the pressure-tube deformation model, lack of capability to adequately predict buoyancy-induced free convection or local steam temperatures, no account for the effects of the increasing flow area resulting from the pressure-tube ballooning on thermalhydraulic and thermal radiation calculations, use of temperature-independent or constant emissivities, and no modelling of axial conduction and radiation. These are the areas where the code can be improved.

## 6. CONCLUSION

CATHENA (MOD-3.3h and 3.4a) were successfully used to perform pre- and post-test analyses of the pressure-tube circumferential temperature

distribution experiment during coolant boil-off. The pre-test simulation results were used to plan the experiment. Extensive post-test comparisons were made between measurement and prediction, and good overall agreement was found. Rupture of the pressure tube did not occur during the experiment and was not predicted in the post-test simulation.

## 7. REFERENCES

- (1) D.J. RICHARDS, B.N. HANNA, N. HOBSON, AND K.H. ARDRON, "CATHENA: A Two-Fluid Code for CANDU LOCA Analysis, (renamed from ATHENA)," Presented at the 3<sup>rd</sup> International Topical Meeting on Reactor Thermalhydraulics, Newport, RI, 1985.
- (2) P.D. LOWE, G.H. ARCHINOFF, J.C. LUXAT, K.E. LOCKE, A.P. MUZUMDAR, C.B. SO, AND R.G. MOYER, "Comparison of Pressure Tube Delta-T Experimental Results with SMARTT Code Predictions," Presented at the 12<sup>th</sup> Annual Symposium on Simulation of Reactor Dynamics and Plant Control, Hamilton, ON, 1986.
- (3) C.B. SO, G.E. GILLESPIE, R.G. MOYER, AND D.G. LIKE, "The Experimental Determination of Circumferential Temperature Distributions Developed in Pressure Tubes During Slow Coolant Boildown," Proceedings of the 8<sup>th</sup> Annual CNS Conference, St. John, NB, 1987.
- (4) P.S. YUEN, K.A. HAUGEN, D.G. LITKE, R.G. MOYER, AND H.E. ROSINGER, "The Experimental Measurement of Circumferential Temperature Distributions Developed on Pressure Tubes Under Stratified Two-Phase Flow Conditions: Tests 1 to 5," Proceedings of the 10<sup>th</sup> Annual CNS Conference, Ottawa, ON, 1989.
- (5) J.P. MALLORY, M.A. WRIGHT, AND H. HUYNH, "Validation of CATHENA at High Temperature Conditions Using CHAN Thermal-Chemical Experimental Results," Presented at the 12<sup>th</sup> Annual CNS Conference, Saskatoon, SK, 1991.
- (6) R.S.W. SHEWFELT AND D.P. GODIN, "Verification Tests for GRAD, A Computer Program to Predict the Nonuniform Deformation and Failure of Zr-2.5 wt% Nb Pressure Tubes During a Postulated Loss-of-Coolant Accident," AECL-8384, 1985.
- (7) F.P. INCROPERA AND D.P. DEWITT, "Fundamentals of Heat and Mass Transfer," 3rd Ed., John Wiley and Sons, pp. 723, 1990.

Table 1  
Summary of Key Results from Experiments and CATHENA Simulations

Description	Experiment S-1-3	Pre-Test Simulation for S-5-1	Experiment S-5-1	Post-Test Simulation for S-5-1
Calandria Tube Inner Diameter (mm)	129.6	136.7	129.6	129.6
Total Electric Power (kW)	85	200	190	190
Total Electric Power per Length (kW/m)	37	111	106	106
Maximum Pressure Tube Heating Rate on Top ( $^{\circ}\text{C}/\text{s}$ )	5.0	5.1	4.0	4.7
Maximum Top-to-Bottom Pressure-Tube Temperature Gradient before Contact ( $^{\circ}\text{C}$ )	590	520	475	513
Maximum Pressure-Tube Temperature prior to Contact ( $^{\circ}\text{C}$ )	751	773	770	769
Initial Pressure-Tube/Calandria-Tube Contact Time (s)	-	-	714	710
Maximum Localized Pressure-Tube Strain near Top (%)	$\infty$	$\infty$	51	59
Time of Pressure-Tube Rupture (s)	696	695	No	No

\* - The start of full power was referenced as time = 480 s

Table 2  
Comparison of Test Sections

	<u>S-1-3</u>	<u>S-5-1</u>
No. of FESs* Heated	36	28
FES OD, mm	13.1	15.2
FES Surface, $\text{m}^2$	3.40	2.41
Heater Core	Zr Tube	Graphite Rod
Heater Insulation	$\text{Al}_2\text{O}_3$ Spacers	$\text{Al}_2\text{O}_3$ Pellets
Heater Length, m	2.3	1.8
FES Mass/Length, $\text{kg}/\text{m}$	7.51	18.38
PT Water Volume, L	18.7	14.5
PT Position in CT	Centre	3.6 mm Low

\* - Fuel Element Simulator

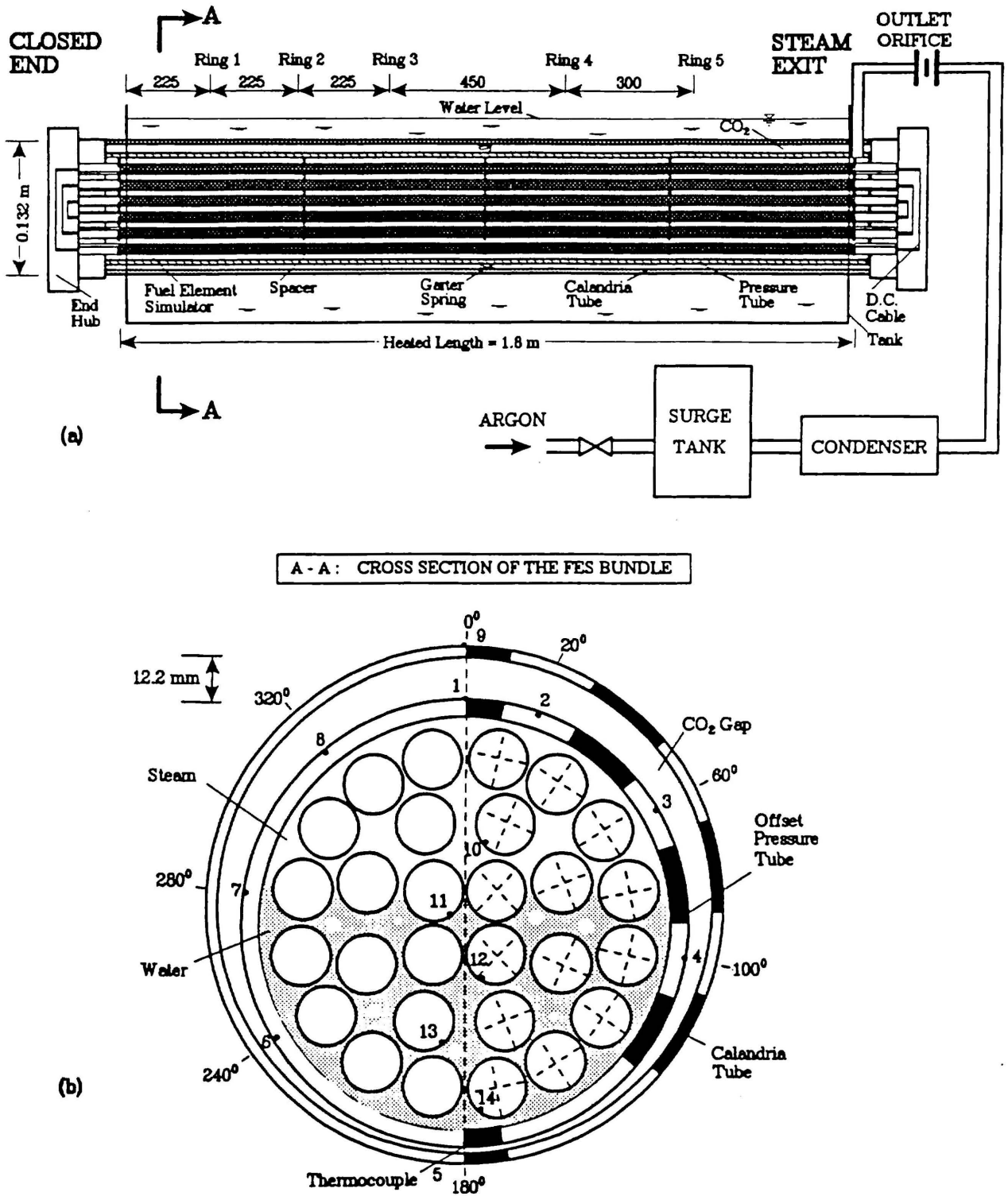
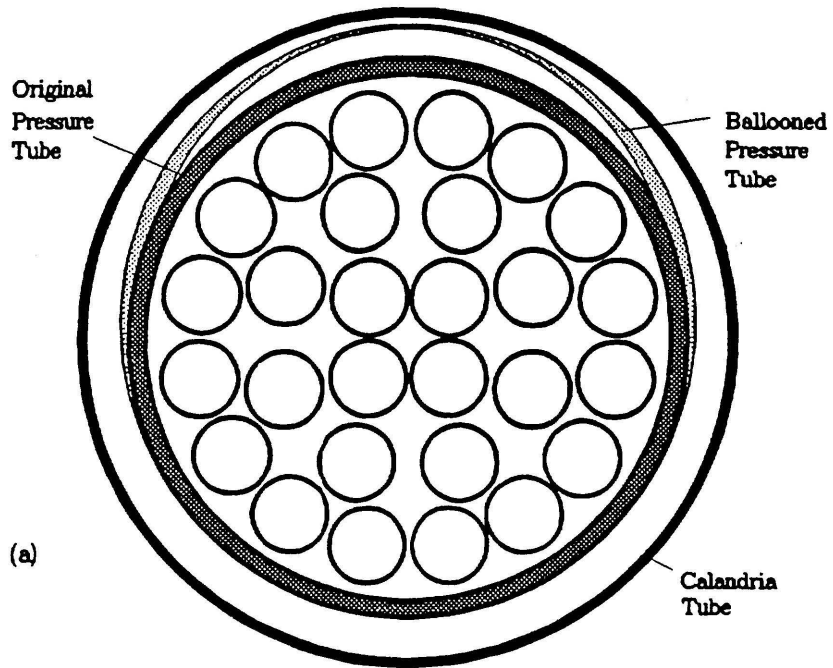


Figure 1: Test Apparatus (a) and the Test Cross Section (b), Showing also CATHENA Sectorization of the Half Channel

### Pressure-Tube Ballooned in an Egg-Shaped Pattern during a Boil-Off Experiment



### CATHENA Idealization of Ballooning

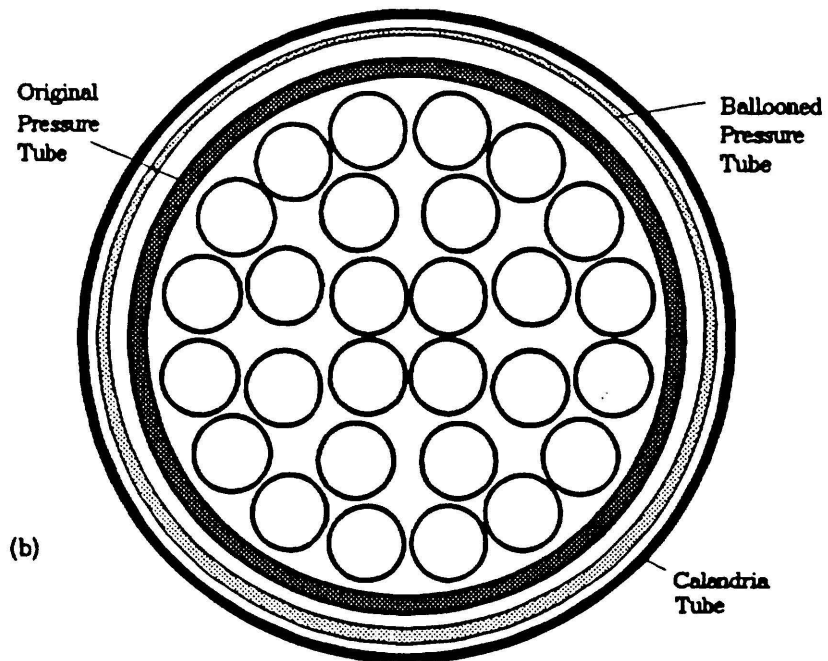


Figure 2: Schematic of Pressure-Tube Ballooning Processes from an Experiment (a) and a CATHENA Simulation (b) When the Pressure Tube is Heated Nonuniformly

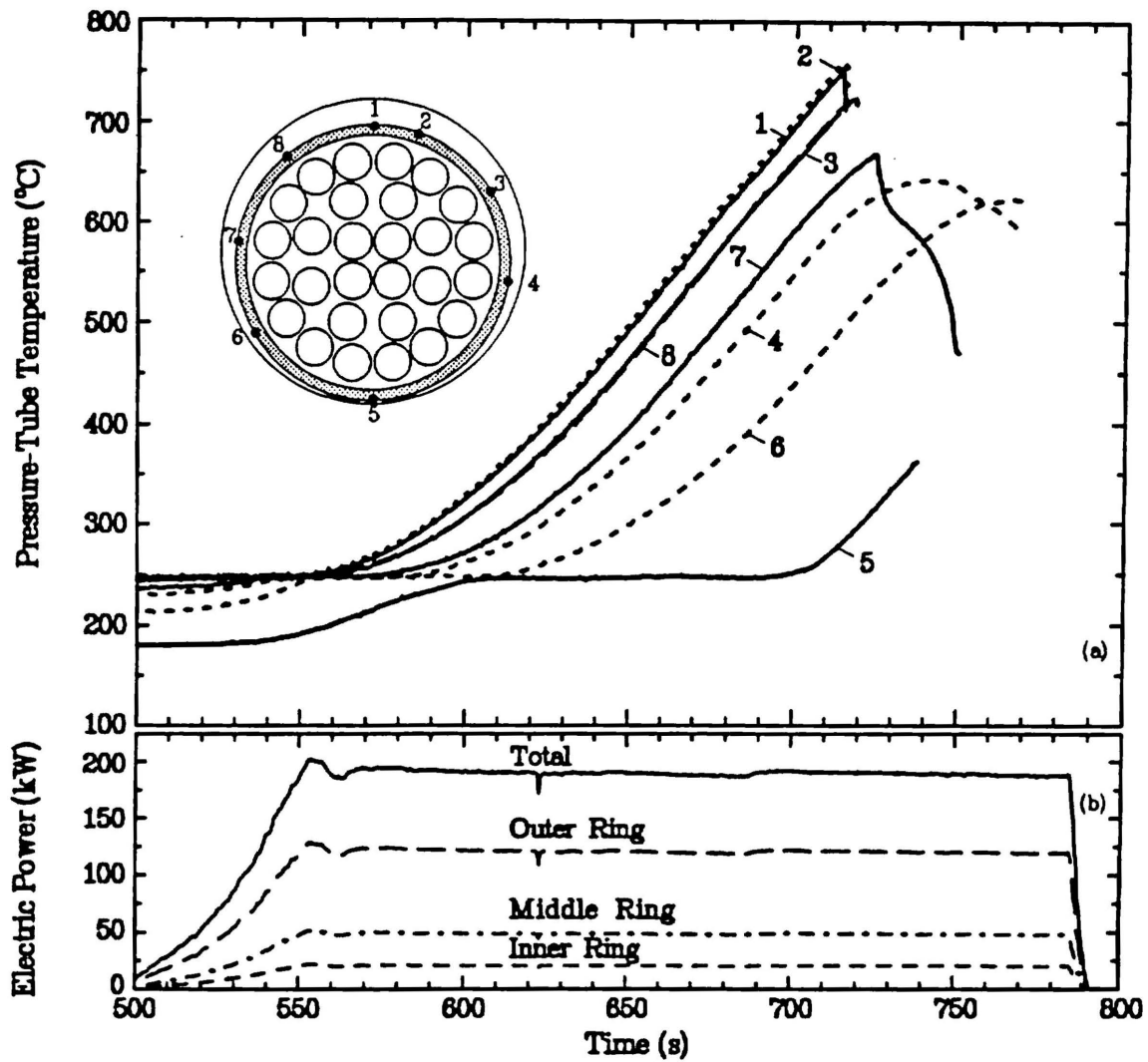


Figure 3: Pressure-Tube Temperatures Measured at Ring 1 - 225 mm from the Closed End (a) and Electric Power (b) during Test S-5-1

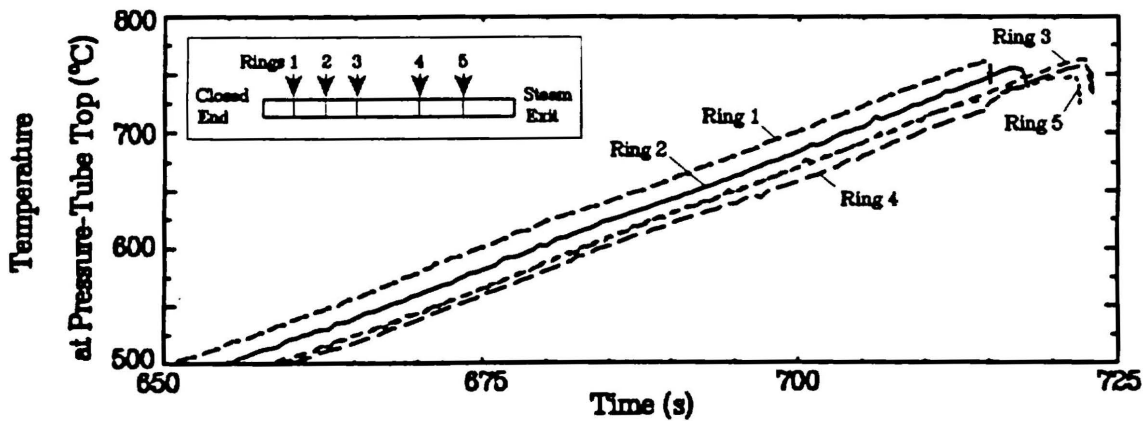


Figure 4: Measured Temperatures near the Pressure Tube Top Showing Axial Variation

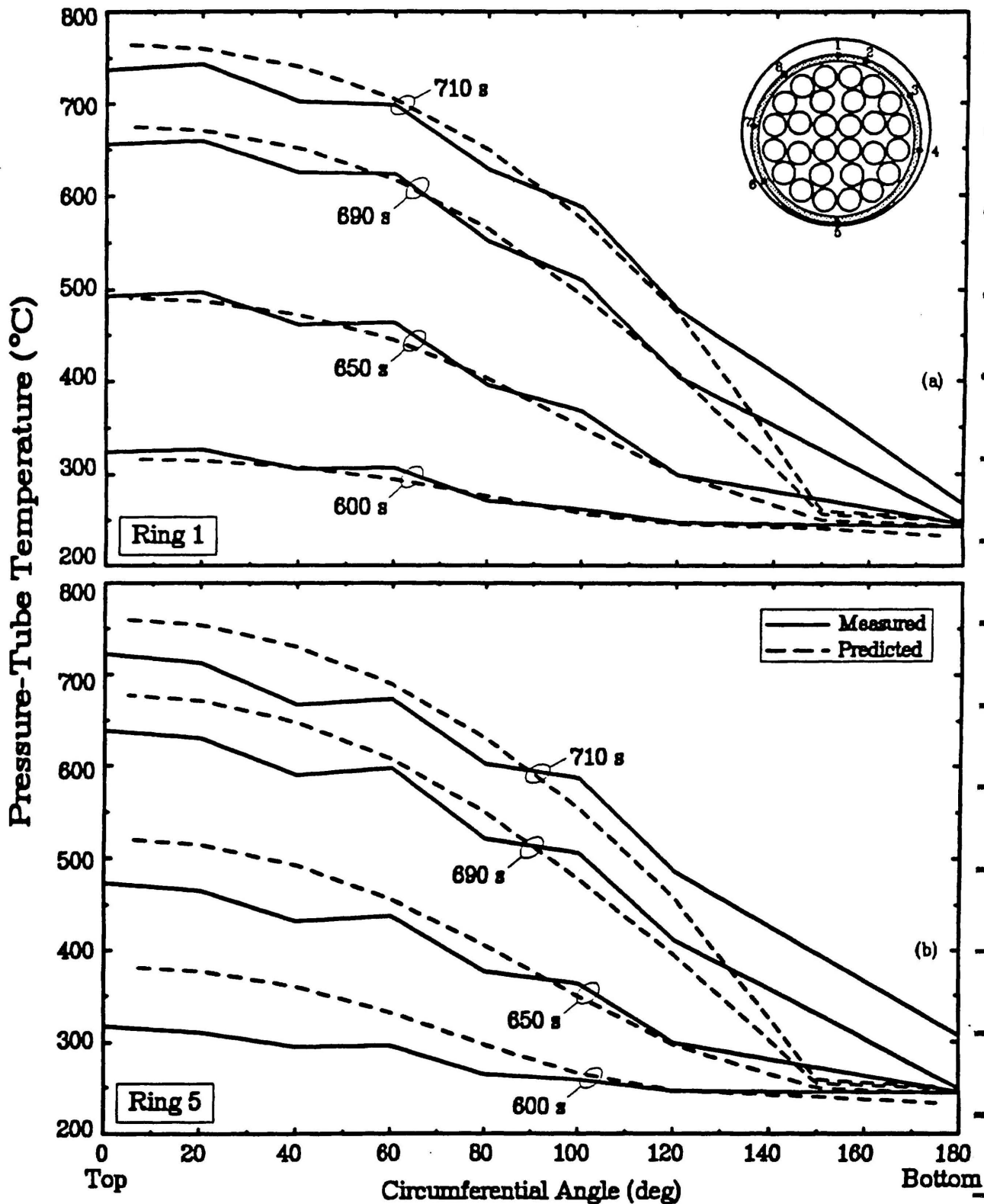
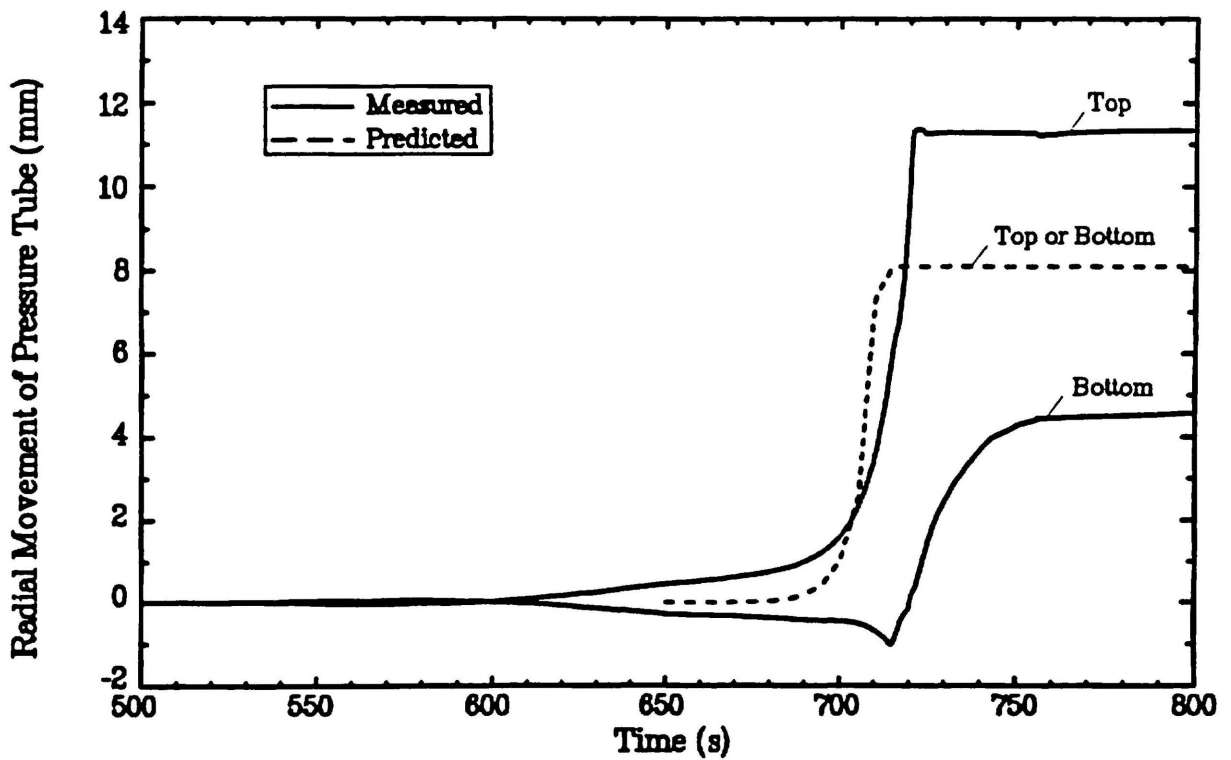
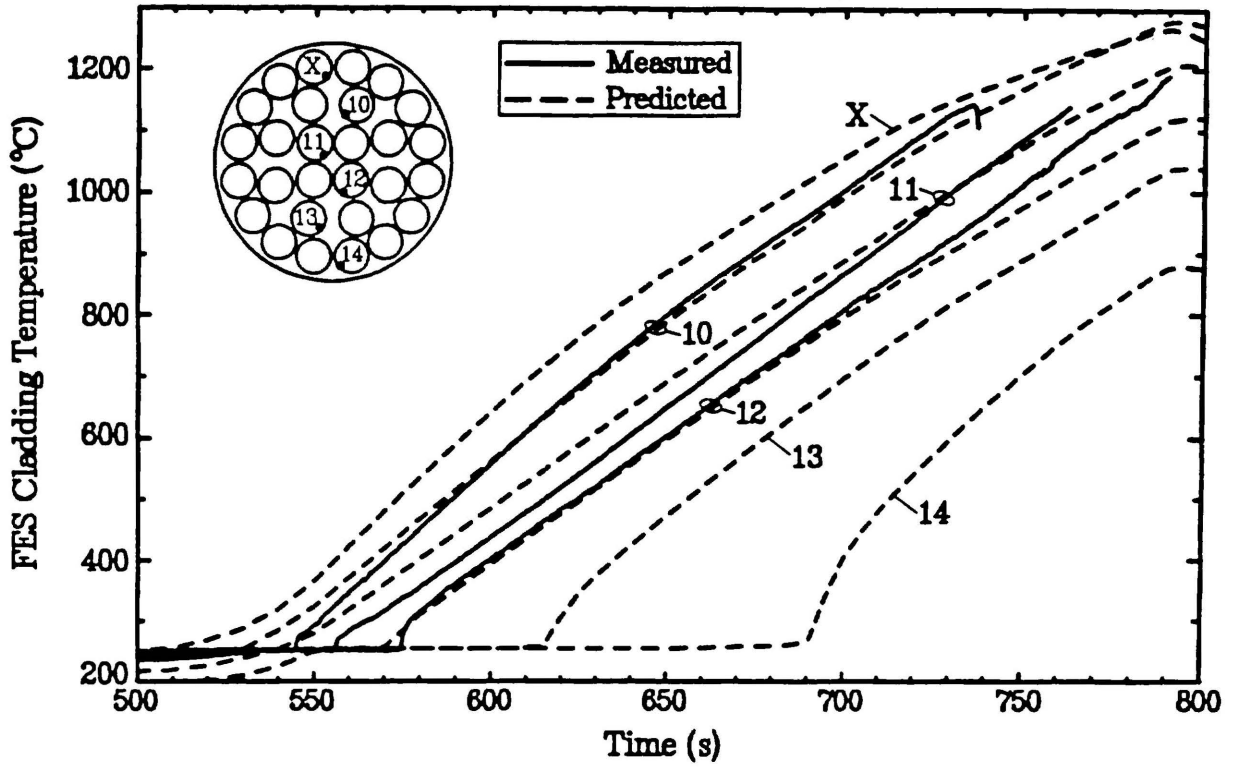


Figure 5: Comparison of Predicted Pressure-Tube Temperature Gradients with Experimental Results of Test S-5-1 at Ring 1 (a) and Ring 5 (b) (225 and 1425 mm from the Closed End) for Four Time Instances



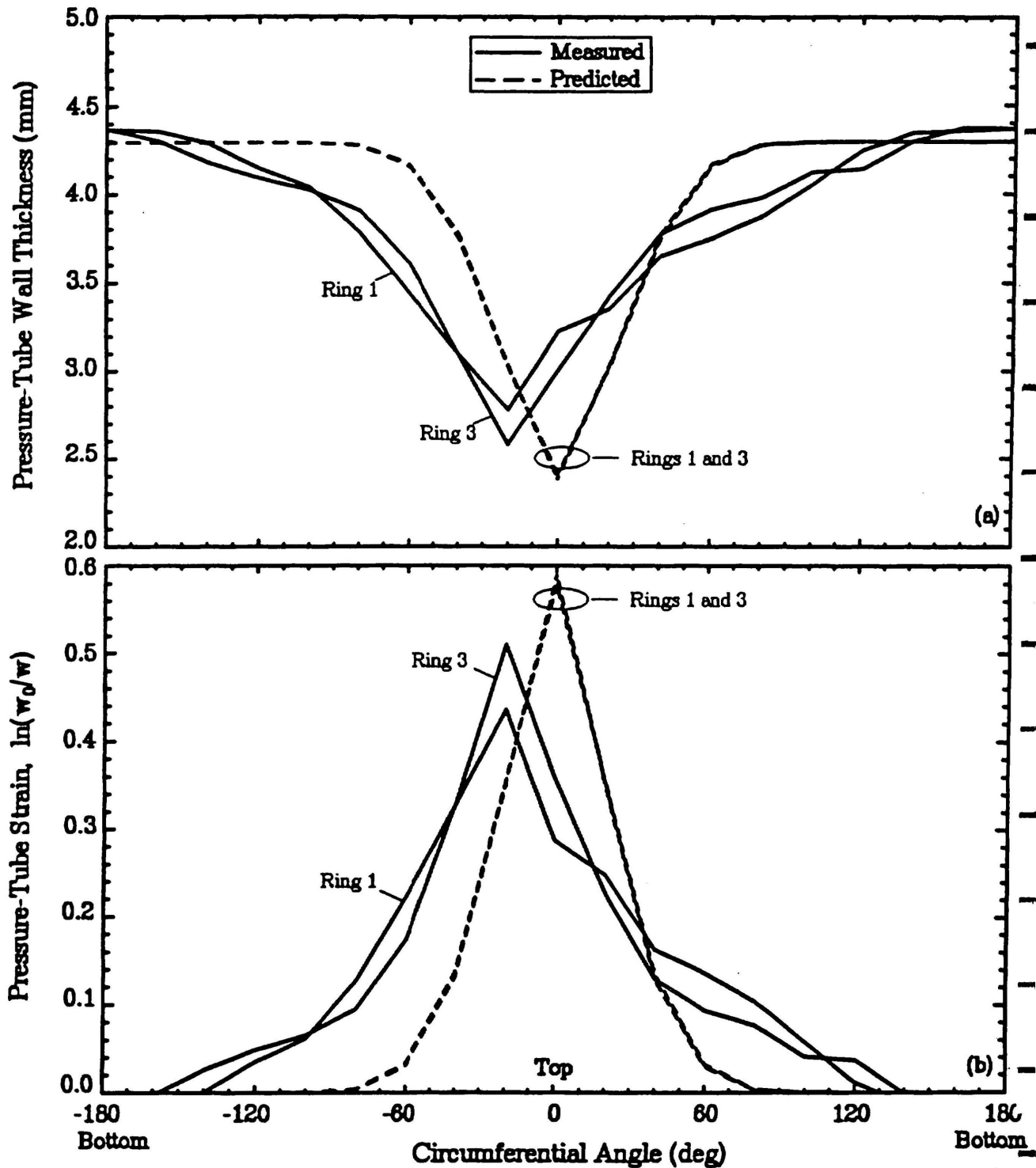


Figure 8: Comparison of CATHENA Predictions with Experimental Results of Test S-5-1: (a) Pressure-Tube Wall Thicknesses and (b) Strains from Post-Test Measurements and at the End of the Simulation for Rings 1 and 3 (225 and 675 mm from the Closed End)

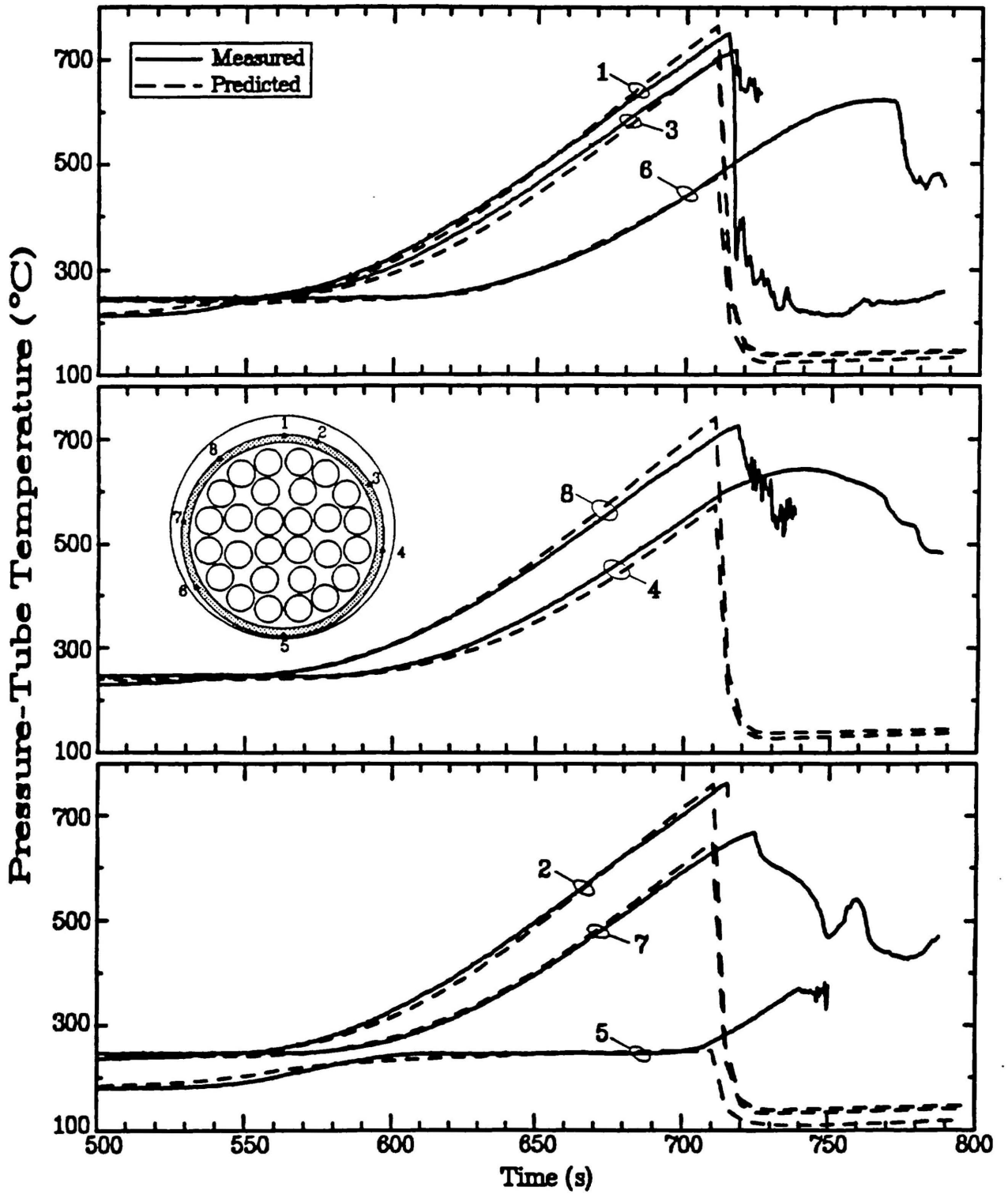


Figure 9: Comparison of Predicted Pressure-Tube Temperatures at Ring 1 (225 mm from the Closed End) with Experimental Results of Test S-5-1

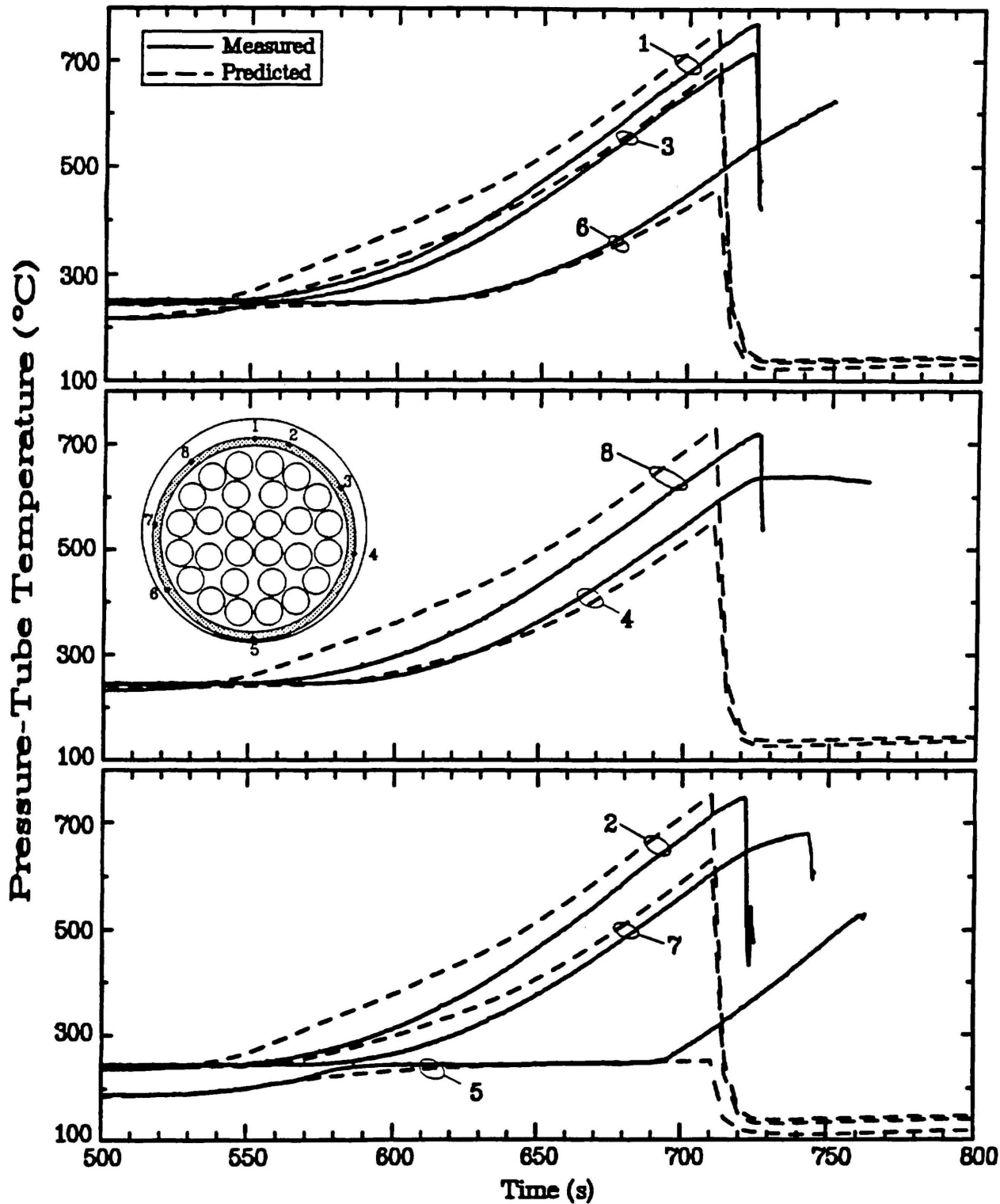


Figure 10: Comparison of Predicted Pressure-Tube Temperatures at Ring 5 (1425 mm from the Closed End) with Experimental Results of Test S-5-1

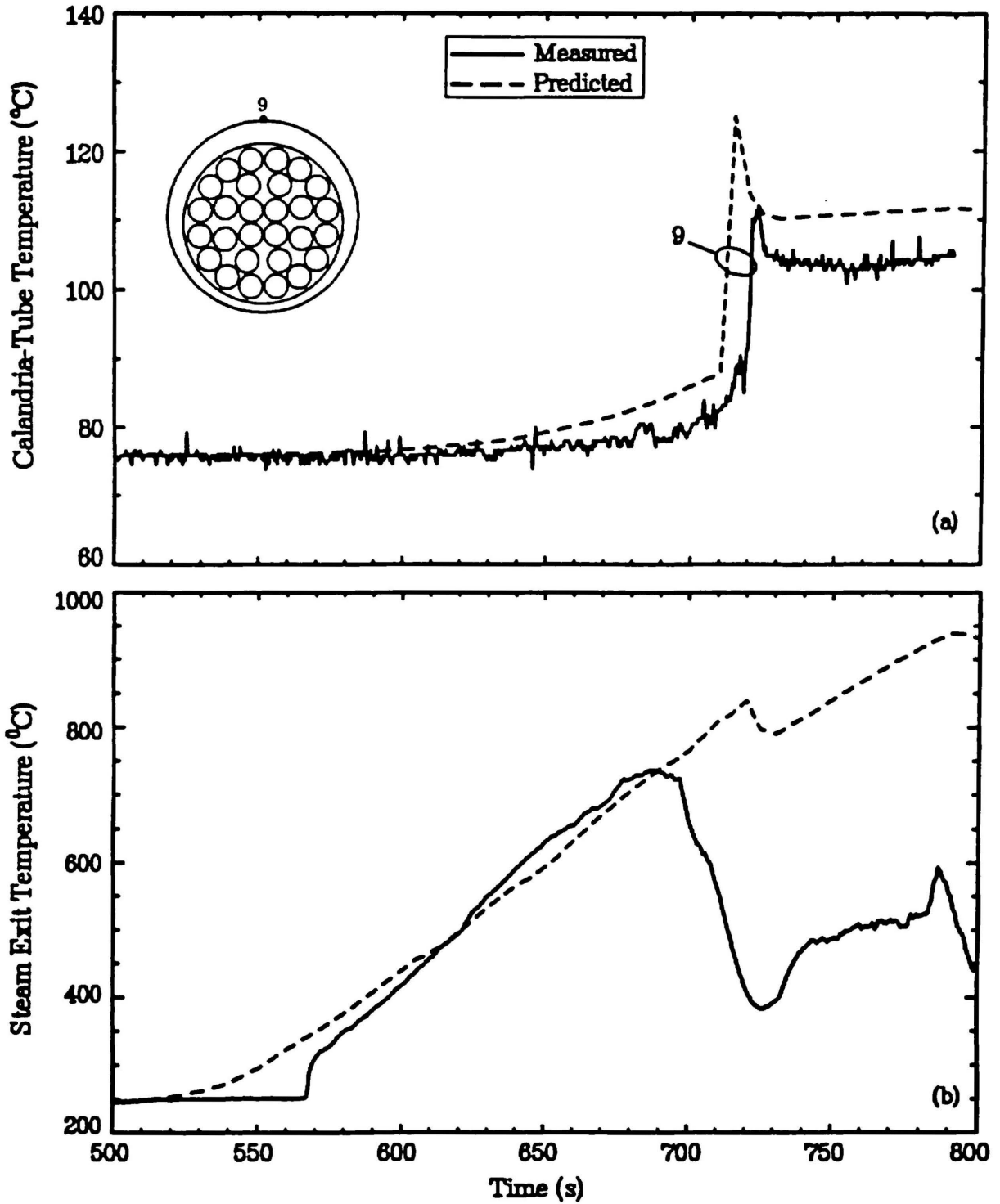


Figure 11: Comparison of CATHENA Predictions with Experimental Results of Test S-5-1:  
(a) Calandria-Tube Temperatures at Ring 1 (225 mm from the Closed End)  
(b) Steam Exit Temperatures